Plant Foods for Human Nutrition (2023) 78:52–60
https://doi.org/10.1007/s11130-022-01021-x

RESEARCH

Functional, Thermal and Structural Properties of Green Banana Flour (cv. Giant Cavendish) by De-astringency, Enzymatic and Hydrothermal Treatments

Hung-Ju Liao[1] · **Chih-Chiao Hung**[1]

Accepted: 17 October 2022 / Published online: 27 October 2022

Abstract
Green banana fruit with high resistant starch (RS) content has a potential to be a nutraceutical ingredient despite having an unpleasant astringency taste and is yet to be fully explored. In this study, the green banana after de-astringency treatment was employed for flour production, and the resulting flour was subjected to modification by the combined treatments of pullulanase debranching and annealing. The banana flour (BF) and the modified flour (MF) were compared with each other by evaluating their functional, thermal and structural properties. The BF showed a restricted-swelling pasting profile, behaving like a slightly chemically cross-linked starch; the MF exhibited less pronounced changes in pasting behavior with increased solubility and decreased swelling power and dispersed volume fraction at elevated temperatures. As compared with the BF, an enhanced thermal stability of the MF was observed, reflected in the endotherm shifting to higher temperatures with increased enthalpy. The BF displayed a C_A-type polymorph, while the MF comprised a mixture of B- and V-type polymorphs with increased crystallinity. The MF showed an increased molecular order, reflected in an increase in short-range double helical order detected in the starch fingerprint regions of FT-IR spectra, and along with increased crystallinity, underlying its enhanced thermal stability. The modification treatment resulted in irregularly shaped flour particles with a more compact structure as revealed by morphological characters. The results of this study can provide useful information for the development of food products using the modified green banana flour with improved thermal stability and functional properties as a health-promoting ingredient.

Keywords Green banana flour · Resistant starch · Functional properties · Long-/short-range order structures

Introduction

Green banana has attracted a great deal of attention recently [1–9], due to a number of beneficial effects on human health, *e.g.*, its physiological fiber-like benefits and improved glycemic and insulinemic responses, a fact often associated with its high level of indigestible carbohydrates, largely resistant starch (RS). Banana is recognized as one of the world's leading food crops cultivated in large quantities in tropical and subtropical areas. About 20% of all bananas harvested become culls during commercialization [10], and attempts are made to use the culled banana for starch production or production of a low-cost banana flour ingredient [11]. Research has been conducted regarding the production of unripe banana flour and its physicochemical, functional, structural and digestion characteristics [9, 12–17]. Although unripe banana exhibits a limited digestibility due to its relatively high RS content, it is worth noting that when cooked its native RS is very likely to be rendered digestible, which poses important limitations to its potential use as a RS source in the formulation of thermally processed foods [18, 19].

RS has been classified into four general subtypes on the basis of the reason for resistance to digestion namely type I (RS_1), physically inaccessible starch; type II (RS_2), native or incompletely gelatinized starch protected from digestion by the conformation or the crystalline structure of granule; type III (RS_3), retrograded starch; and type IV (RS_4), chemically modified starch [20]. Retrograded amylose, short linear

✉ Hung-Ju Liao
markliao@mail.ncyu.edu.tw

[1] Department of Food Science, National Chiayi University, No. 300 Syuefu Road, Chiayi City 600355, Taiwan, Republic of China

segments of α-1, 4 polyglucans re-associating as double helices packed into crystalline arrays, is produced by starch gelatinization and subsequent retrogradation, a slow re-crystallization of starch components upon cooling. Formation of these structures is influenced by amylose content, polymer chain length, process conditions affecting crystallization process such as water content of starch gel, process temperature and time with respect to nucleation and propagation, and the presence of other components associated strongly to amylose [21]. Enzymatic debranching with pullulanase (EC 3.2.1.41), which can cleave α-1,6 glucosidic bonds from the amylopectin molecule and give rise to linear glucans that can more readily re-associate, has been employed to further increase RS_3 formation [22]. Chain-length distribution analysis revealed that banana starch contained long outer amylopectin α-1, 6-linked side chains and seemed to be an excellent source for the production of RS_3 [22].

Flour production instead of starch isolation from green banana fruit can be cost-effective for obtaining a promising functional ingredient [10]. Banana flour is a good source of several health-promoting ingredients, such as RS_2, dietary fiber and antioxidant polyphenol [23]. Based on the low-cost production and the health-promoting benefits, green banana flour can be a better alternative to banana starch. Green banana flour can also compete with corn starch due to the lack of characteristics of native corn starch, e.g., thermal- and shear-induced loss of thickening power, which often requires further modification [10, 19]. Green banana flour has unpleasant astringency taste due to the presence of the soluble condensed tannins, and RS_2 in green banana flour is thermally unstable. Our previous study has successfully employed limewater for de-astringency of the green banana flour tannin [21]. Little is known regarding RS_3 formation from de-astringent green banana flour and its functional and structural characteristics. In a previous publication from our laboratory [21], we described observations of chemical compositions and *in vitro* starch hydrolysis kinetics of de-astringent green banana flour and its RS_3 product. We showed that the rate and extent of starch hydrolysis and the glycemic response were different between the RS_3 product and its parental flour, and the type and amount of RS in these flours had an obvious impact on duration of the glycemic response. To expand the study, the present work aimed to evaluate the functional and structural characteristics of green banana flour and its modified flour by enzymatic and hydrothermal treatments.

Materials and Methods

This section was described in the Supplementary Material.

Results and Discussion

Pasting Properties

Typical RVA pasting profiles of the GBF and the MF at 4, 7 and 10% concentrations are illustrated in Fig. 1, and the corresponding pasting data are given in Table 1. The GBF and the MF, containing predominantly starch (68.6 and 67.4%, respectively), largely in the form of RS (30.3 and 25.3%, respectively), exhibited variable pasting behaviors. The pasting temperature (PT) was 76.5–77.1℃ in the GBF, resembling the temperature range of banana starch (*Musa* sp.) reported previously [24]. It showed that swollen granules of the GBF apparently resisted breakdown with slight decrease in viscosity during the 95℃ hold (Fig. 1). This corroborates previous findings [19, 24] that green banana starch granules belonged to the restricted-swelling type with good stability, behaving in ways that are somewhat similar to a slightly chemically cross-linked starch. Restricted-type

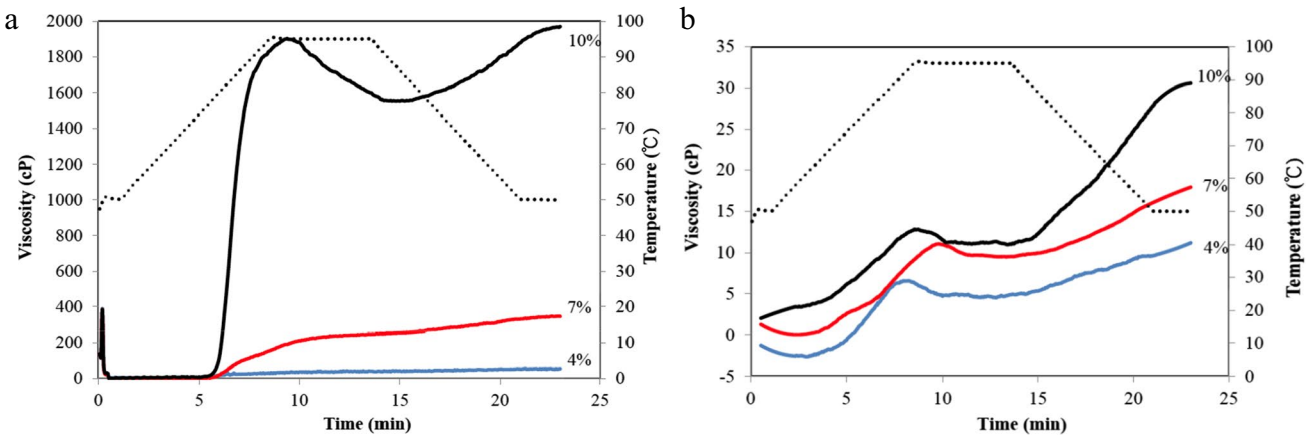

Fig. 1 Typical pasting profiles of the GBF (**a**) and the MF (**b**) at concentrations of 4, 7 and 10%

Table 1 Pasting characteristics of the GBF and the MF

Sample	PT (°C)	PV (cP)	HPV (cP)	BD (cP)	CPV (cP)	SB (cP)
GBF						
4%	77.1 ± 1.1 [a]	35 ± 10 [a]	33 ± 9 [a]	2 ± 1 [a]	51 ± 5 [a]	19 ± 1 [a]
7%	76.5 ± 0.2 [a]	236 ± 12 [b]	234 ± 11 [b]	2 ± 1 [a]	328 ± 25 [b]	94 ± 13 [b]
10%	77.0 ± 0.3 [a]	1887 ± 21[c]	1504 ± 69 [c]	384 ± 47 [b]	1949 ± 30 [c]	445 ± 38 [c]
MF						
4%	N.D	7 ± 2 [d]	5 ± 2 [d]	2 ± 0 [a]	11 ± 2 [d]	6 ± 1 [d]
7%	N.D	12 ± 3 [e]	10 ± 2 [e]	2 ± 1 [a]	16 ± 2 [e]	6 ± 1 [d]
10%	N.D	13 ± 2 [e]	11 ± 2 [e]	2 ± 1 [a]	31 ± 5 [f]	20 ± 2 [a]

Data are means ± SD; $n = 3$. Means with different superscript letters withing the same column differed significantly ($p < 0.05$)

Parameters are obtained from Rapid Visco-Analyzer

N.D.: not detected. PT: pasting temperature; PV: peak viscosity; HPV: hot paste viscosity; BD: breaddown viscosity (=PV-HPV); CPV: cool paste viscosity; SB: setback (=CPV-HPV)

swelling pattern and a high pasting temperature suggest strong bonding forces within the starch granule of the GBF. The pasting behavior of the MF was less pronounced than that of its parental flour with no detectable pasting temperature; the pasting viscosities including peak viscosity, hot paste viscosity and cold paste viscosity were much lower for the MF than for its parental flour. These results suggest that a substantially higher amount of thermally stable double helical crystallites in the MF was responsible for its resistance to swelling and melting compared to its parental flour, in agreement with previous research [21]. A decrease in breakdown viscosity for the MF reflects that the structure of the MF was thermally highly stable, whereas a marked decrease in setback viscosity provides the evidence that the chain length of the glucan molecules in the MF could no longer be suitable to form double helical crystallites.

Swelling Power, Solubility and Dispersed Volume Fraction

The swelling power (G) and solubility (S) of the flours at 1% concentration during heating from 30 to 90℃ are presented in Fig. 2a and b, respectively. The swelling-solubility behavior of the flours was strongly associated with temperature. The swelling power and solubility values of the GBF remained fairly unchanged at 30–70℃, but increased rapidly during heating at 80 and 90℃. This can be ascribed to the high amounts of starch in the GBF undergoing gelatinization, thus permitting progressive water flux into granules with concomitant swelling and amylose solubilization after the onset temperature was reached, in rather good agreement with the pasting temperature range obtained from the RVA experiments. The swelling-solubility patterns and values of the GBF were comparable to those reported previously for banana starch by Kayisu et al. [25] who suggested the swelling and solubility values of banana starch were comparatively lower than those of other starches, reflecting a more ordered, more strongly bonded and denser structure within banana starch granule. The swelling power values of the MF remained constant at 30–50℃, similar to those of its native counterpart, and started to increase at temperatures above 60℃. The increases, however, were less pronounced for the MF than for its parental flour, suggesting that at the elevated temperatures less water was absorbed into the particles of the MF indicative of excellent heat resistance due to greater crystalline areas along with stronger bonds in the crystalline domains as a result of retrogradation (Fig. 2a). The solubility values of the MF increased with temperature and were much higher than those of its parental flour over the temperature range investigated (Fig. 2b). These results reconfirm the evidence for the presence of high levels of thermally stable RS_3 and soluble linear α-glucan in the MF.

It has been proposed by Bagley and Christianson [26] that, in excess water, volume fraction of the swollen particles in the dispersion can be estimated from cQ:

$$cQ = (1 - \frac{S}{100}) \times c \times G$$

where c is concentration of the flour and expressed in g/g. Figure 2c illustrates the cQ values of the GBF and the MF at 1% concentration during heating from 30 to 90℃. The cQ values of the GBF and the MF (range, 0.034–0.132 and 0.031–0.034, respectively) were far less than unity during heating at 30–90℃, suggesting that the volume fraction occupied by the dispersed phase of deformable particles of swollen and fragmented granules still left enough space for the particles to swell freely (Fig. 2c). The cQ values of the GBF remained nearly constant until 80℃, and started to increase rapidly thereafter, a fact associated with starch gelatinization in the GBF treated at that temperature; such a pattern resembles that obtained for swelling power, thus expressing the close link between these two phenomena.

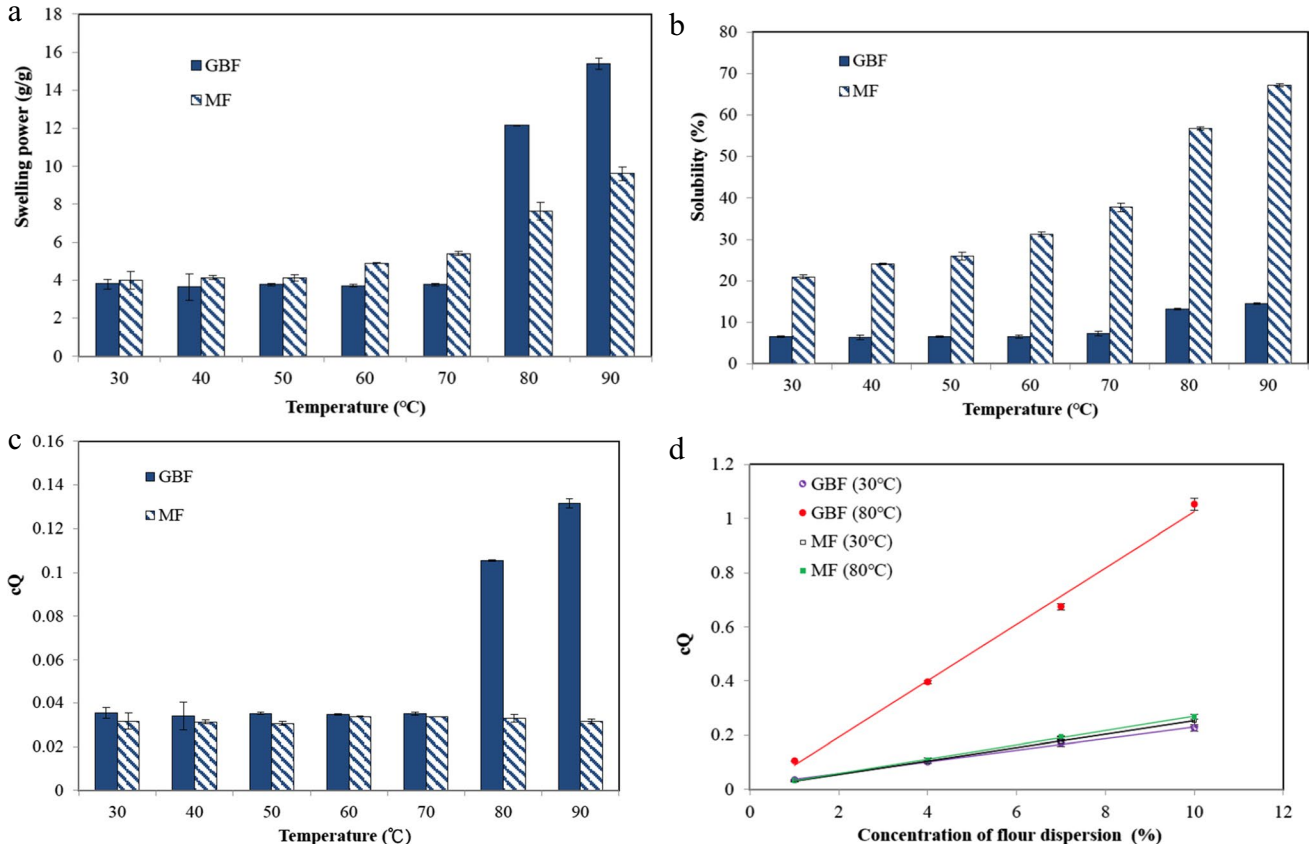

Fig. 2 Swelling power (**a**), solubility (**b**) and cQ (**c**) at 1% concentration during heating at 30–90℃, and variation of cQ with concentrations at 30 and 80℃ (**d**) of the GBF and the MF. Error bars show ± SD ($n = 3$)

Contrastingly, the cQ values of the MF were almost independent of the temperature, and remained low and fairly constant at 30–90℃ (Fig. 2c), suggesting the dispersion with the MF comprised a more rigid dispersed phase during heating due to the more strongly bonded and denser structure within the particles. Figure 2d shows variation of the cQ values with concentration for the GBF and the MF during heating at 30 and 80℃. The results suggested that the volume fractions occupied by swollen particles increased linearly with concentration. From the linear relation shown, the cQ corresponding to the 10% GBF when heated at 80℃ approximately equaled to unity. Thus, 10% can be considered as the concentration for which the GBF paste was just full of closely packed swollen particles at that temperature. At the same concentration the cQ values of the GBF when heated at 80℃ were higher than those of the GBF when heated at 30℃ and those of the MF when heated at 30 and 80℃, indicating that the MF was superior to its parental flour for its rigidity and thermal resistance as a potentially important RS source in the formulation of thermally processed foods.

DSC Thermograms

Typical DSC thermograms of the GBF and the MF are shown in Fig. 3a, and the corresponding thermal parameters are given in Table 2. The GBF exhibited the endotherm between 75.3 (initial temperature, T_o) and 87.0℃ (conclusion temperature, T_c) with peak temperature (T_p) of 80.2℃ and enthalpy (ΔH) of 8.0 J/g due to the starch gelatinization process (Fig. 3a). No phase transition below 100℃ was detected for the MF (Fig. 3a), indicating that the starch granules in the MF were fully gelatinized and completely ruptured during the preparation. The MF exhibited the endothermic transition between 132.0 (T_o) and 143.5℃ (T_c) with peak temperature of 136.3℃ and enthalpy of 29.9 J/g, which was assigned to the melting of double helical crystallites. It has been reported that the endothermic peak in the temperature range 120–165℃ was associated with the melting of amylose double helices [27]. These results verify the suitability of the MF for commercial food application under high-temperature processing due

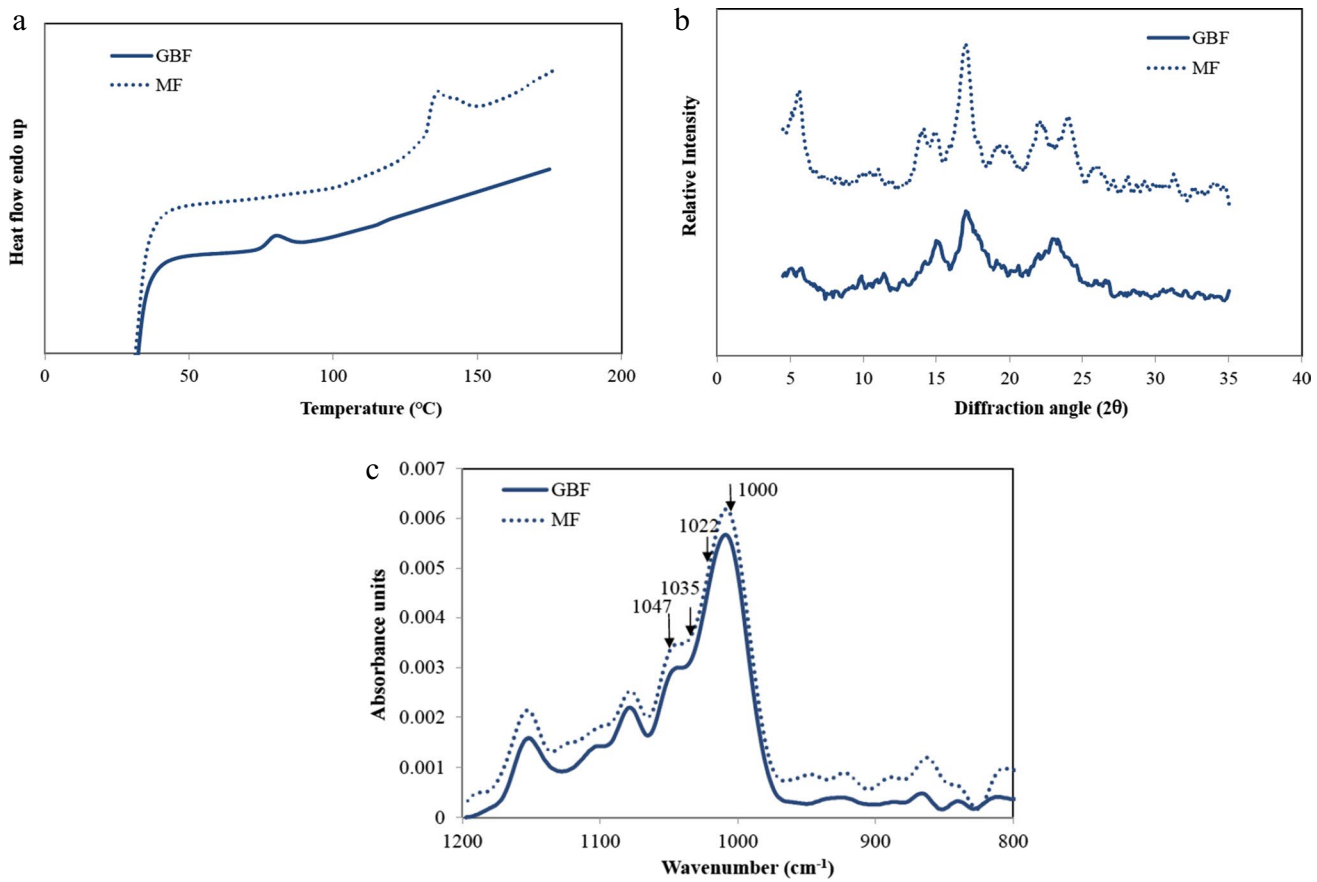

Fig. 3 Typical DSC thermograms (**a**), FTIR spectra (**b**) and X-ray diffractograms (**c**) of the GBF and the MF

Table 2 Thermal parameters from DSC thermograms, level of crystallinity from the X-ray diffractograms and molecular order from the FT-IR spectra of the GBF and the MF

	GBF	MF
DSC		
T_0 (°C)	75.3 ± 0.4 [a]	132.0 ± 5.1 [b]
T_P (°C)	80.2 ± 1.0[a]	136.3 ± 3.3[b]
T_C (°C)	87.0 ± 1.0 [a]	143.5 ± 4.5 [b]
ΔH (J/g)	8.0 ± 0.5 [a]	29.9 ± 1.1 [b]
XRD		
Crystallinity (%)	13.2 ± 0.4 [a]	17.9 ± 0.1 [b]
Polymorph type	C_A	B + V
FT-IR		
Ratio 1047/1022 cm^{-1}	0.68 ± 0.01 [a]	0.73 ± 0.01 [b]
Ratio 1047/1035 cm^{-1}	0.88 ± 0.01 [a]	0.94 ± 0.01[b]
Ratio 1000/1022 cm^{-1}	0.90 ± 0.06 [a]	1.15 ± 0.03 [b]

Data are means ± SD, $n = 3$. Means with different superscript letters within the same row differed significantly ($p < 0.05$)

T_0: onset temperature; T_P: peak temperature; T_C: conclusion temperature; ΔH: enthalpy of the thermal transition

to its higher thermal stability and resistance to enzymatic hydrolysis.

XRD Patterns

X-ray diffraction pattern reflects starch long-range order such as the packing of double helices into a periodic array called a crystalline lattice [28]. Typical X-ray diffractograms of the GBF and the MF are presented in Fig. 3b, and the corresponding levels of crystallinity are shown in Table 2. The X-ray pattern of the GBF was characterized by strong reflections at 15.0 and 17.0° (2θ), a very broad reflection centered at 23.3° (2θ) and a weak B-type signature reflection at 5.4° (2θ). This revealed the GBF consisted of mixed crystals of A-type and B-type polymorphs but bearing a close resemblance to A-type, a pattern referred to as C_A-type, in agreement with the results observed by Pelissari et al. [28] for the "Terra" variety banana flour. Contrastingly, diffraction pattern of the MF was clearly distinct from that of its native counterpart, with the increased intensities of the B-type polymorph signature reflection at 5.4° (2θ) and the reflection at 17.0° (2θ), the replacement of the reflections at 15.0 and 23.3° (2θ) by unresolved doublets at 14.1–15.0°

(2θ) and at 22.0–24.0º (2θ), respectively, and the appearance of a conspicuous new reflection peak at 20.0º (2θ), indicating changes in the lattice structure during the process for obtaining RS. As for the MF, the signature reflections at 5.4º (2θ) implied presence of B-type pattern and the reflection at 20.0º (2θ) reflected V-type crystallinity, associated with ordered single-helical amylose or amylose complexed with lipids (Fig. 3b), but this kind of crystallinity is also characterized by another reflections at 7 and 13º (2θ) [29], which were conspicuously absent in the diffractograms of the MF. As a consequence, the MF was ascribed to a mixture of B- and V-crystalline types. Similar pattern was also observed in the RS product obtained from starches/flours from different botanical sources treated with pullulanase followed by retrogradation at low temperature [30, 31]. The crystallinity values were estimated as 13.2 and 17.9% for the GBF and the MF, respectively (Table 2). The crystallinity of 13.2% corresponded approximately with literature values [28]. An increase in the crystallinity of the MF implied the structural reorganization encouraging crystal formation and growth, and coincided with its high thermal stability.

FT-IR Spectra

Figure 3c shows the FT-IR spectra in the starch fingerprint region 800–1200 cm^{-1} for the GBF and the MF and Table 2 presents their absorbance ratios 1047/1022, 1047/1035 and 1000/1022 cm^{-1}. The infrared spectrum in the starch fingerprint region 800–1200 cm^{-1} was proposed to be sensitive to changes in short-range structural order, in which local ordered domains exist, such as chain conformation and helicity, as distinct from the long-range order with packing of double helices into ordered crystalline arrays detected by X-ray diffraction [32]. The ratios of the absorbance of the specific bands of infrared spectra of starch samples have been used to express the amount of short-range order: the ratio 1047/1022 cm^{-1}, where the absorption bands at 1047 and 1022 cm^{-1} are respectively associated to crystalline domains and amorphous contribution, and the ratio 1047/1035 cm^{-1}, where the valley at 1035 cm^{-1} is the characteristic of the presence of short-range order. [32]; the former ratio has been used to express the amount of starch crystalline domains to amorphous contribution, whereas the latter ratio is just a measure of the amount of starch crystalline domains [32]. Moreover, the increase of the ratio 1000/1022 cm^{-1} has been thought to characterize double helices reaching a more ordered structure [29].

As illustrated in Fig. 3c, the MF shows an increase in the absorbance of the bands at 1000 and 1047 cm^{-1} with more pronounced increase at 1000 cm^{-1}, but a similar absorbance of the band at 1022 cm^{-1}, as compared to its parental flour. This suggests that the MF underwent double helices reorganization during the preparation with much more extensive and stronger intramolecular hydrogen bonding of hydroxyl groups in the crystal domains than its parental counterpart. The absorbance ratios 1047/1022, 1047/1035 and 1000/1022 cm^{-1} of the GBF and the MF are presented in Table 2, where it can be observed that the MF shows a slight, albeit significant, increase in the absorbance ratios 1047/1022 and 1047/1035 cm^{-1}, and a pronounced increase in the absorbance ratio 1000/1022 cm^{-1}, as compared to its parental counterpart. This indicates that the MF not only had significantly higher amounts of short-range order but also exhibited a more ordered structure of double helices than its parental counterpart, which could account for its enhanced thermal stability and enzyme resistance.

Morphological Features

The SEM micrographs of the GBF and the MF are shown in Fig. 4. SEM studies revealed that the GBF is mostly composed of starch granules and a substantial amount of cell wall material (Fig. 4a1 and a2). The material adhering to the surface of the granules is most likely to be amyloplast membranes, which enclose starch granules in the banana fruit cell. The banana starch granule is highly irregular in shape and size and ranged from oval to elongated oval forms (Fig. 4a1), as reported previously [10]. The surface of the granules was uneven with small depressions (see arrows in Fig. 4a1 and a2), revealing that some areas were easier to hydrolyze than others. This is in line with previous research [17], which suggested that although the banana fruits were in a mature-green stage, surface degradation of the granule starch had already been initiated by hydrolytic enzymes but it has not been established yet which structural property of the banana starch granule is responsible for its resistance to enzymatic attack. The granules appeared to be intact, without fractures, suggesting the adequacy of the process used to obtain the flour. The SEM micrographs (Fig. 4b1 and b2) of the MF resemble irregularly shaped particles with some remnants of cell wall material and a more compact, layered and plate-like structure, leading to the loss of the distinct morphological appearance of native granules, in good agreement with previous research [33]. The change in appearance from granules to irregularly shaped particles is due to the consequence of autoclaving and pullulanase debranching where the linear α-glucans with the optimum chain lengths form double helices packing to a more compact structure of the retrograded amylose during recrystallization. This change in the more compact structure leads to highly thermally stable and resistant to the attack of amylolytic enzyme on the MF particles.

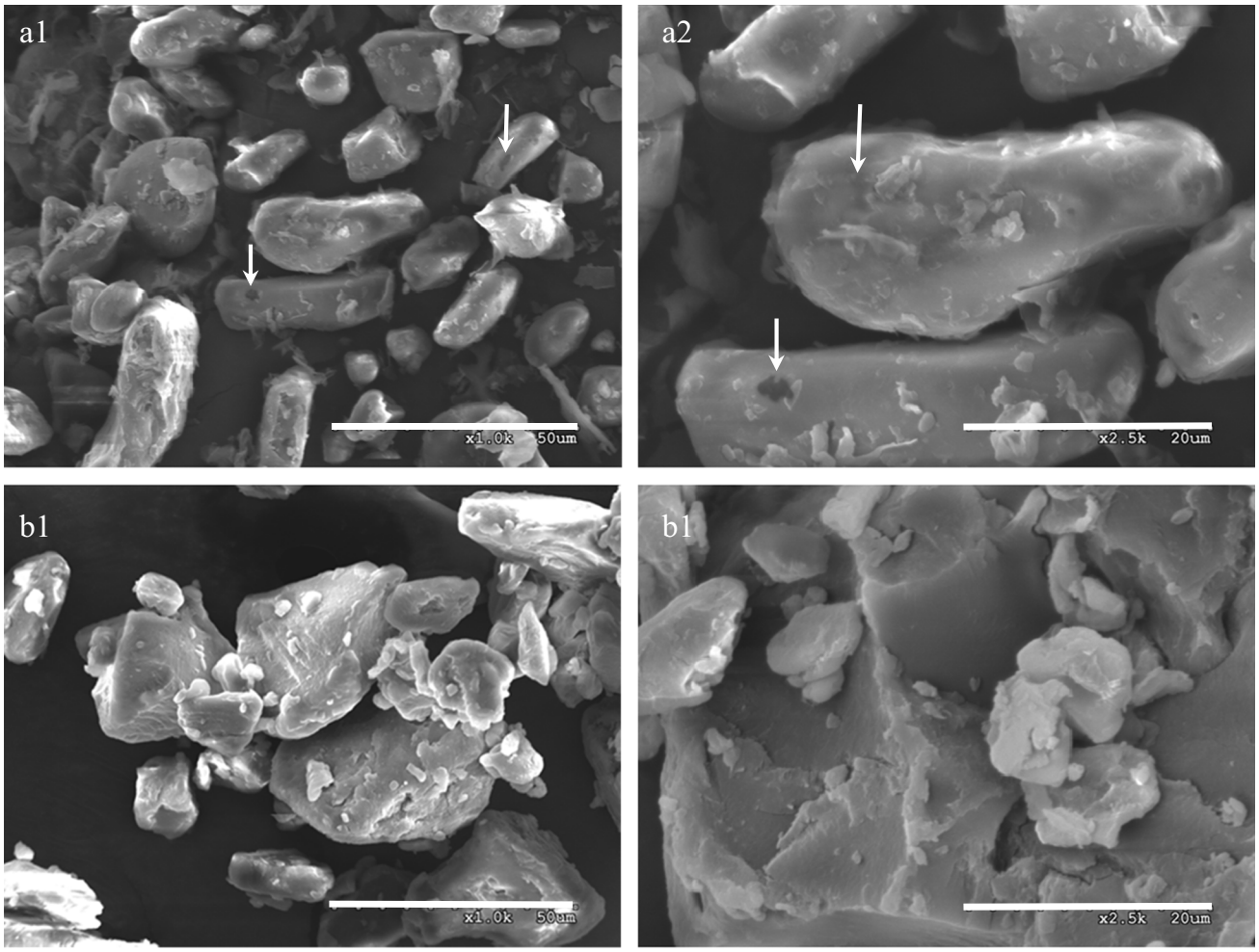

Fig. 4 Typical SEM images of the GBF (**a**) and the MF (**b**) at 1000X magnification (bar = 50 ·m) (1) and 2500X magnification (bar = 20 ·m) (2). The pictures (a1 and a2) show native green banana flour is mostly composed of intact starch granules with depressions (see arrows) and a large amount of cell wall material

Conclusions

This study has shown that the de-astringent green banana flour when subjected to pullulanase debranching and hydrothermal treatments resulted in the formation of a RS-rich powder with less pronounced changes in pasting behavior, decreased swelling power and volume fraction of dispersed phase, and increased solubility, due to the increased levels of soluble glucans and RS_3. The enzymatic debranching of banana amylopectin led to the formation of linear short chain molecules, and the hydrothermal treatment (annealing) was beneficial for the linear chain rearrangement in favor of the formation of double helical crystallites. The modification process led to changes in the crystallinity pattern from C_A-type polymorph to a mixture of B- and V-type polymorphs and increases in the crystallinity. The modified flour when compared with its native counterpart have shown a better thermal stability and the potential to reduce the pasting viscosity as a result of increased crystallinity and molecular order due to the double helices reorganization during the retrogradation process. The long- and short-range structural features underlying the increased thermal stability of the modified flour relative to its parental counterpart had a major impact on the duration of the glycemic response. Our study can provide useful information for the development of food products using the modified green banana flour with improved thermal stability and functional properties as a health-promoting ingredient, especially suitable for incorporating the modified banana flour into the formulation of thermally processed foods such as canned foods and baking products.

Supplementary Information The online version contains supplementary material available at https://doi.org/10.1007/s11130-022-01021-x.

Authors' Contributions The authors confirm contribution to the paper as follows: study conception and design, analysis and interpretation of

results, and draft manuscript preparation: Hung-Ju Liao; data collection: Chih-Chiao Hung. All authors reviewed the results and approved the final version of the manuscript.

Funding The partial financial support by Council of Agriculture of the Republic of China, Taiwan, in the publication of the finished report is greatly appreciated (Grant No. 99–3.1.4-Z1(3)).

Data Availability Data are available from the corresponding author.

Declarations

Ethics Approval Not applicable.

Consent to Participate Not applicable.

Consent for Publication Not applicable.

Conflict of Interest/Competing Interests Authors declare no conflict of interest.

References

1. Ahmed J, Thomas L, Khashawi R (2020) Influence of hot-air drying and freeze-drying on functional, rheological, structural and dielectric properties of green banana flour and dispersions. Food Hydrocoll 99:105331
2. Cahyana Y, Wijaya E, Halimah TS et al (2019) The effect of different thermal modifications on slowly digestible starch and physicochemical properties of green banana flour (*Musa acuminata* colla). Food Chem 274:274–280
3. de Barros HEA, Natarelli CVL, de Abreu DJM et al (2021) Application of chemometric tools in the development of food bars based on cocoa shell, soy flour and green banana flour. Int J Food Sci Technol 56:5296–5304
4. Harastani R, James LJ, Ghosh S et al (2021) Reformulation of muffins using inulin and green banana flour: physical, sensory, nutritional and shelf-life properties. Foods 10:1883
5. Radünz M, Camargo TM, Nunes CFP et al (2021) Gluten-free green banana flour muffins: chemical, physical, antioxidant, digestibility and sensory analysis. J Food Sci Technol 58:1295–1301
6. Khoza M, Kayitesi E, Dlamini BC (2021) Physicochemical characteristics, microstructure and health promoting properties of green banana flour. Foods 10:2894
7. Kumar PS, Saravanan A, Sheeba N et al (2019) Structural, functional characterization and physicochemical properties of green banana flour from dessert and plantain bananas (*Musa* spp.). LWT-Food Sci Technol 116:108524
8. Rachman A, Brennan MA, Morton J et al (2021) Starch pasting properties, and the effects of banana flour and cassava flour addition to semolina flour on starch and amino acid digestion. Starke 73:2000137
9. Rodrígues-Damian AR, De La Rosa-Millán J, Agama-Acevedo E et al (2013) Effect of different thermal treatments and storage on starch digestibility and physicochemical characteristics of unripe banana flour. J Food Process Preserv 37:987–998
10. Zhang P, Whistler RL, BeMiller JN et al (2005) Banana starch: production, physicochemical properties, and digestibility—a review. Carbohydr Polym 59:443–458
11. Nasrin TAA, Anal AK (2014) Resistant starch III from culled banana and its functional properties in fish oil emulsion. Food Hydrocoll 35:403–409
12. Bezerra CV, Amante ER, de Oliveira DC et al (2013) Green banana (*Musa cavendishii*) flour obtained in spouted bed– effect of drying on physico-chemical, functional and morphological characteristics of the starch. Ind Crops Prod 41:241–249
13. de la Rosa-Millán J, Agama-Acevedo E, Osorio-Díaz P et al (2014) Effect of cooking, annealing and storage on starch digestibility and physicochemical characteristics of unripe banana flour. Rev Mex Ing Quim 13:151–163
14. De La Rosa-Millán J, Lin AH-M, Osorio-Díaz P et al (2015) Influence of annealing flours from raw and pre-cooked plantain fruit on cooked starch digestion rates. Starke 67:139–146
15. Giraldo-Toro A, Gibert O, Ricci J et al (2015) Digestibility prediction of cooked plantain flour as a function of water content and temperature. Carbohydr Polym 118:257–265
16. Langkilde AM, Champ M, Andersson H (2002) Effects of high-resistant-starch banana flour (RS2) on *in vitro* fermentation and the small-bowel excretion of energy, nutrients, and sterols: an ileostomy study. Am J Clin Nutr 75:104–111
17. Menezes EW, Tadini CC, Tribess TB et al (2011) Chemical composition and nutritional value of unripe banana flour (*Musa acuminata*, var. Nanicão). Plant Foods Hum Nutr 66:231–237
18. Rodríguez-Ambriz SL, Islas-Hernández JJ, Agama-Acevedo E et al (2008) Characterization of a fibre-rich powder prepared by liquefaction of unripe banana flour. Food Chem 107:1515–1521
19. Zhang P, Hamaker BR (2012) Banana starch structure and digestibility. Carbohydr Polym 87:1552–1558
20. Englyst HN, Kingman SM, Cummings JH (1992) Classification and measurement of nutritionally important starch fractions. Eur J Clin Nutr 46:S33-50
21. Liao H-J, Hung C-C (2015) Chemical composition and *in vitro* starch digestibility of green banana (cv. Giant Cavendish) flour and its derived autoclaved/debranched powder. LWT-Food Sci Technol 64:639–644
22. Lehmann U, Jacobasch G, Schmiedl D (2002) Characterization of resistant starch type III from banana (*Musa acuminata*). J Agric Food Chem 50:5236–5240
23. Pelissari FM, Andrade-Mahecha MM, Sobral PJdA et al (2012) Isolation and characterization of the flour and starch of plantain bananas (*Musa paradisiaca*). Starke 64:382–391
24. Lii C-Y, Chang S-M, Young Y-L (1982) Investigation of the physical and chemical properties of banana starches. J Food Sci 47:1493–1497
25. Kayisu K, Hood LF, Vansoest PJ (1981) Characterization of starch and fiber of banana fruit. J Food Sci 46:1885–1890
26. Bagley EB, Christianson DD (1982) Swelling capacity of starch and its relationship to suspension viscosity-effect of cooking time, temperature and concentration. J Texture Stud 13:115–126
27. Haralampu SG (2000) Resistant starch—a review of the physical properties and biological impact of RS_3. Carbohydr Polym 41:285–292
28. Sevenou O, Hill SE, Farhat IA et al (2002) Organisation of the external region of the starch granule as determined by infrared spectroscopy. Int J Biol Macromol 31:79–85
29. Lopez-Rubio A, Flanagan BM, Shrestha AK et al (2008) Molecular rearrangement of starch during *in vitro* digestion: toward a better understanding of enzyme resistant starch formation in processed starches. Biomacromol 9:1951–1958
30. Shi M-M, Chen Y, Yu S-J et al (2013) Preparation and properties of RS III from waxy maize starch with pullulanase. Food Hydrocoll 33:19–25
31. Shi M-M, Gao Q-Y (2011) Physicochemical properties, structure and *in vitro* digestion of resistant starch from waxy rice starch. Carbohydr Polym 84:1151–1157
32. van Soest JJG, Tournois H, de Wit D et al (1995) Short-range structure in (partially) crystalline potato starch determined with

attenuated total reflectance Fourier-transform IR spectroscopy. Carbohydr Res 279:201–214
33. Zhang H, Jin Z (2011) Preparation of products rich in resistant starch from maize starch by an enzymatic method. Carbohydr Polym 86:1610–1614